

RESEARCH

Open Access



Establishment of multiplex RT-PCR to detect fusion genes for the diagnosis of Ewing sarcoma

Hitomi Ueno-Yokohata^{1*}, Hajime Okita^{1,2,3,4*}, Keiko Nakasato¹, Chikako Kiyotani⁵, Motohiro Kato^{5,6}, Kimikazu Matsumoto⁵, Nobutaka Kiyokawa¹, Atsuko Nakazawa⁷ and Takako Yoshioka⁴

Abstract

Background: Detection of the tumor-specific *EWSR1/FUS-ETS* fusion gene is essential to diagnose Ewing sarcoma. Reverse transcription–polymerase chain reaction (RT–PCR) and fluorescence in situ hybridization are commonly used to detect the fusion gene, and assays using next-generation sequencing have recently been reported. However, at least 28 fusion transcript variants have been reported, making rapid and accurate detection difficult.

Methods: We constructed two sets of multiplex PCR assays and evaluated their utility using cell lines and clinical samples.

Results: *EWSR1/FUS-ETS* was detected in five of six tumors by the first set, and in all six tumors by the second set. The fusion gene detected only by the latter was *EWSR1-ERG*, which completely lacked exon 7 of *EWSR1*. The fusion had a short N-terminal region of *EWSR1* and showed pathologically atypical features.

Conclusions: We developed multiplex RT–PCR assays to detect *EWSR1-ETS* and *FUS-ETS* simultaneously. These assays will aid the rapid and accurate diagnosis of Ewing sarcoma. In addition, variants of *EWSR1/FUS-ETS* with a short N-terminal region that may have been previously missed can be easily detected.

Keywords: Ewing sarcoma, Multiplex RT–PCR, Genetic diagnosis, Fusion gene, *EWSR1*, Transcription factor, Breakpoint

Background

Ewing sarcoma primarily occurs in the bones and soft tissues of children and young adults. It is characterized by fusion genes between a gene of the RNA-binding FET family (*EWSR1* or *FUS*) with a gene of the ETS-transcription factor family (*FLII*, *ERG*, *ETV1*, *ETV4* (*E1AF*), and *FEV*) [1–5], which are called *EWSR1/FUS-ETS* fusion genes. *EWSR1-FLII*, generated by t(11;22)(q24.3;q12.2), occurs most frequently, followed by *EWSR1-ERG*, which is generated by t(21;22)(q22.2;q12.2)

[6]. Similarly, *EWSR1-ETV1*, *EWSR1-ETV4*, *EWSR1-FEV*, *FUS-ERG*, and *FUS-FEV* are rarely formed in Ewing sarcoma, and these are generated by t(7;22)(p21.2;q12.2), t(17;22)(q21.31;q12.2), t(2;22)(q35;q12.2), t(16;21)(p11.2;q22.2) and t(2;16)(q35;p11.2), respectively [7, 8]. Additionally, various exon combinations exist in *EWSR1/FUS-ETS* fusion genes. In *EWSR1-FLII*, the combination of *EWSR1* exon 7 and *FLII* exon 6 occurs most commonly, followed by the combination of *EWSR1* exon 7 and *FLII* exon 5. *EWSR1* exon 7 and *ERG* exon 7 or *EWSR1* exon 7 and *ERG* exon 9 are common exon combinations in *EWSR1-ERG*. These fusion genes contain the ETS consensus sequence in-frame [9, 10]. The conserved ETS consensus sequence recognizes the ETS

* Correspondence: ueno-ht@ncchd.go.jp; okita-h@keio.jp

¹Department of Pediatric Hematology and Oncology Research, National Research Institute for Child Health and Development, Tokyo 157-8535, Japan
Full list of author information is available at the end of the article



© The Author(s). 2021 **Open Access** This article is licensed under a Creative Commons Attribution 4.0 International License, which permits use, sharing, adaptation, distribution and reproduction in any medium or format, as long as you give appropriate credit to the original author(s) and the source, provide a link to the Creative Commons licence, and indicate if changes were made. The images or other third party material in this article are included in the article's Creative Commons licence, unless indicated otherwise in a credit line to the material. If material is not included in the article's Creative Commons licence and your intended use is not permitted by statutory regulation or exceeds the permitted use, you will need to obtain permission directly from the copyright holder. To view a copy of this licence, visit <http://creativecommons.org/licenses/by/4.0/>. The Creative Commons Public Domain Dedication waiver (<http://creativecommons.org/publicdomain/zero/1.0/>) applies to the data made available in this article, unless otherwise stated in a credit line to the data.

motif, competes with wild type ETS-transcription factors, and consequently contributes to Ewing tumorigenesis [11].

Ewing sarcoma is composed of dense and diffuse proliferation of small round blue cells with fine chromatin [12]. Generally, it lacks immunohistochemical evidence of differentiation lineages, such as muscle, bone, cartilage, fibroblast and endothelium. Diffuse membranous CD99 immunoreactivity is a hallmark of this tumor and more than 90% of tumors were reported to have *EWSRI/FUS-ETS*. Therefore, detection of the fusion gene is important to diagnose Ewing sarcoma. Fluorescence in situ hybridization (FISH), reverse transcription-polymerase chain reaction (RT-PCR), including multiplexed assay, and targeted next-generation sequencing have been reported. FISH using an *EWSRI* or a *FUS* break-apart probe is commonly used in clinical settings, but FISH using formalin-fixed paraffin-embedded tissue may sometimes be challenging [13]. Additionally, fusion partners cannot be determined by a single break-apart assay. Many tumors, such as desmoplastic small round cell tumor, myxoid liposarcoma, clear cell sarcoma of tendons and aponeuroses, angiomatoid fibrous histiocytoma, and myoepithelioma, have a fusion gene related to *EWSRI* and *FUS* [14–18]. Therefore, we believe that the determination of the fusion partner gene is important for the differential diagnosis. RT-PCR detection is sensitive and specific, and it can determine the fusion partner. However, assays for seven different fusion genes are needed for Ewing sarcoma. Multiplex RT-PCR assay is an efficient technique. Nevertheless, multiplex RT-PCR assays for *EWSRI-ETS* have been reported, those for both *EWSRI-ETS* and *FUS-ETS* fusion genes have not [19–22]. Next-generation sequencing is a robust technique, but it is too expensive. Therefore, we aimed to create a multiplex RT-PCR system that can simultaneously detect known *EWSRI/FUS-ETS* fusion genes. Moreover, we confirmed the utility using clinical samples and plasmids.

Materials and methods

Clinical samples

The pathological diagnosis was confirmed by H.O., A.N., and/or T.Y. based on morphological observations and existing RT-PCR and/or FISH analysis. The clinical samples other than tumor 4 used in this study had already been identified for fusion variants by existing RT-PCR. Furthermore, the multiplex RT-PCR and sequencing analysis were performed as blind for experimenter, and the result was collated with that of existing method. Immunostaining was performed using HISTOSTAINER (NICHIREI BIOSCIENCES, Tokyo, Japan) or the BOND-III automated stainer (Leica Biosystems, Nussloch, Germany). Detailed information about the

antibodies used in this study is listed in Supplementary Table S1.

RT-PCR

Tumor tissue for genetic analyses was evaluated by frozen sections, and neoplastic cells accounted for 30–80% of viable cells. The total tumor RNA was extracted using the RNeasy Mini kit (Qiagen, Hilden, Germany), according to the manufacturers' protocols. The concentrations of DNA and RNA were assessed using an absorption spectrometer. NCR-EW2, WES, and NCR-EW3 are Ewing sarcoma cell lines, and express *EWSRI-FLII* (fusion variant 8 in Fig. 1), *EWSRI-ERG* (fusion variant 19 in Fig. 1) and *EWSRI-ETV4* (fusion variant 22 in Fig. 1), respectively [23]. NRS-1 (rhabdomyosarcoma cell line) and HEK293 total RNA were used as negative controls [24]. Total RNA was extracted from cells using ISOGEN (NIPPON GENE CO., LTD., Tokyo, Japan). The entire coding sequences of the *EWSRI-ETVI*, *EWSRI-FEV*, *FUS-ERG*, and *FUS-FEV* were constructed and subcloned into the pGEM-T vector (Promega, Madison, WI). The exon combinations of the control plasmids were *EWSRI* (NM_001163285.2) exon 7 – *ETVI* (NM_001163148.1) exon 11 (fusion variant 21 in Fig. 1), *EWSRI* exon 10 – *FEV* (NM_017521.2) exon 2 (fusion variant 23 in Fig. 1), *FUS* (NM_004960.3) exon 7 – *ERG* exon 11 (fusion variant 25 in Fig. 1), and *FUS* exon 10 – *FEV* exon 2 (fusion variant 28 in Fig. 1), respectively. Reverse transcription was performed using the Transcriptor First Strand cDNA Synthesis Kit with Oligo dT primers and random hexamers (Roche Diagnostics, Mannheim, Germany). The reaction temperature and time were applied in accordance with the protocol for long length mRNA recommended by the manufacturer's protocol. Multiplex RT-PCR was performed using the Qiagen Multiplex PCR Plus Kit (Qiagen, Hilden, Germany). Conventional RT-PCR was performed using the QIAGEN HotStarTaq Plus Master Mix Kit (Qiagen, Hilden, Germany). Two sets of primers for multiplex RT-PCR were designed to detect fusion transcript variants. The primers are shown in Table 1. β -Actin primers used as the control were described elsewhere [25]. NCBI Primer-BLAST (<https://www.ncbi.nlm.nih.gov/tools/primer-blast/>) was used to design the primers, and the search conditions were set, so that the T_m of the primers was within $60 \pm 3^\circ\text{C}$, the maximum T_m difference was within 3°C and an amplicon of the longest variant was within 1000 bp for Set A. As the forward primer of Set B, the most suitable primer was selected in combination with all reverse primers. It was confirmed by the Multiplex Primer Analyzer (Thermo Fisher SCIENTIFIC) that dimer formation did not theoretically occur in multiplex method. The optimal conditions for multiplex RT-PCR were as follows (based on the

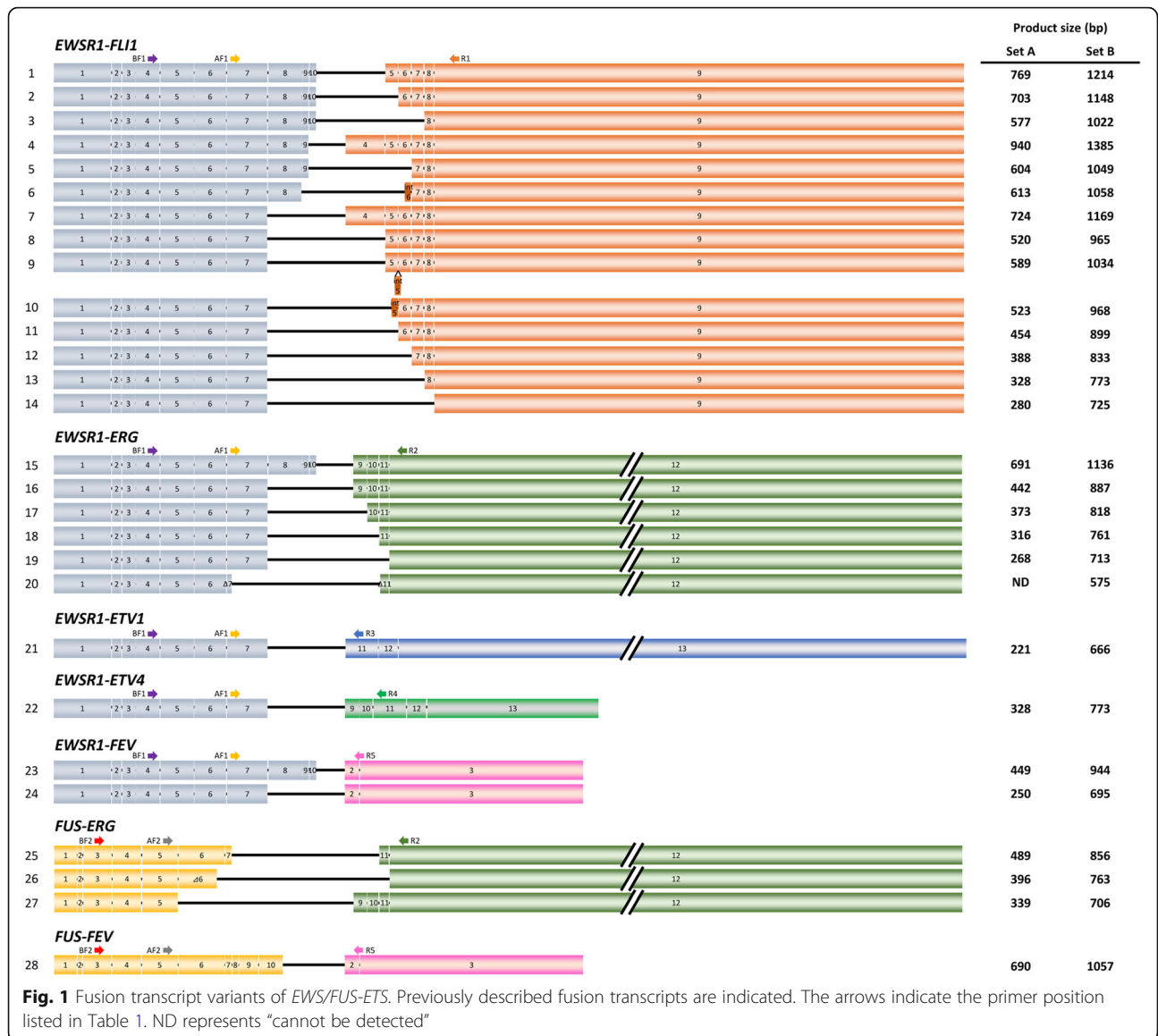


Table 1 Primer sequences for multiplex RT-PCR

Primer name	5' ----- 3'	RT-PCR		Sequencing		
		Set A	Set B	F mix (set A)	F mix (set B)	R mix
EWSR1ex7_F (AF1)	gaacacctatgggcaaccga	✓		✓		
EWSR1ex4_F (BF1)	agaccgcctatgcaacttct		✓		✓	
FLI1ex9_R (R1)	ctcatcggggtccgctattt	✓	✓			✓
ERGex12_R (R2)	cgctcatctggaactccccgt	✓	✓			✓
ETV1ex11_R (R3)	atcctcggcttggtatgtg	✓	✓			✓
ETV4ex11_R (R4)	gaccccttctgcttgatgt	✓	✓			✓
FEVex2/3_R (R5)	gatctgtccgctgctttct	✓	✓			✓
FUSex5_F (AF2)	ggacagcagaaccagtacaaca	✓		✓		
FUSex3_F (BF2)	cggacagcagagttacagtgg		✓		✓	

recommendation by the manufacturer's protocol): final concentration of each primer is 0.2 μ M, initial PCR activation at 95 °C for 5 min, 30–40 cycles of PCR consisting of denaturation at 95 °C for 30 s, annealing at 60 °C for 90 s and extension at 72 °C for 90 s, and final extension at 68 °C for 10 min. RT–PCR products of Set A and Set B were detected by electrophoresis using 2 and 1% agarose gel/ 1 \times TAE buffer, respectively.

Genomic PCR

The tumor genomic DNA was extracted using the QIAamp DNA Mini kit (Qiagen, Hilden, Germany), according to the manufacturers' protocol. Genomic PCR was performed using AccuPrime Taq DNA Polymerase, high-fidelity (Invitrogen, Carlsbad, CA). The primers are listed in Supplementary Table S2.

Sequencing analyses

Sequencing analysis was performed using ABI3130xl and ABI3500 (Applied Biosystems, Foster City, CA). The sequencing of the multiplex RT–PCR product was also performed using multiplex primers with 3.2 p mol each primer.

Results

Generation of the multiplex RT–PCR method to detect EWSR1/FUS-ETS

Design of the multiplex RT–PCR primers

We aimed to set up a multiplex RT–PCR system to detect all *EWSR1/FUS-ETS* fusion variants for rapid and practical genetic diagnosis. However, the exon combinations of the fusion gene are quite broad, and at least 28 types of variants have been reported (Fig. 1) [3, 5, 7–10, 23, 26–28]. There are 14 reported exon combinations of *EWSR1-FLII*, all of which include exon 7 of *EWSR1*. Six combinations were reported in *EWSR1-ERG*. Five of them contained the complete exon 7 of *EWSR1*, whereas a single case only partially contained exon 7 [27]. One type of each was reported for *EWSR1-ETV1* and *EWSR1-ETV4*. Two types were reported for *EWSR1-FEV*. In summary, *EWSR1-ETS* contained the entire exon 7 of *EWSR1* except for one case. Therefore, a forward primer was designed to bind exon 7 of *EWSR1* as primer Set A. Reverse primers were designed to bind a common region in each fusion gene; that is, an *FLII* primer was designed for exon 9, an *ERG* primer for exon 12, an *ETV1* primer for exon 11, and an *ETV4* primer for exon 11. The *FEV* primer spanned exon 2 to exon 3. Among *FUS-ERG* and *FUS-FEV* variants, the variant that fuses *FUS* exon 5 to *ERG* exon 9 has the shortest 5'-terminal side sequences of *FUS*. Therefore, a forward primer was designed in exon 5. Because all *FUS-ERG* variants include exon 12 of *ERG*, and *FUS-FEV* variants include exon 2 of *FEV*, the same reverse primers for

EWSR1-ETS were used. The deduced size of each PCR product was 221 to 940 base pairs.

Next, we generated primer Set B that could detect fusion with a shorter 5'-terminal side sequence. The *EWSR1* forward primer was designed within exon 4 to detect the fusion gene that partially lacks exon 7. The *FUS* forward primer was designed within exon 3 to detect unusually short fusion genes, although no fusion with a shorter *FUS* 5'-terminal side sequence were reported in Ewing sarcoma. These forward primers were designed to match the reverse primer of Set A. Set A primers detect most variants, and the Set B primers cover all variants reported thus far (Table 1).

Sensitivity for the detection of EWSR1/FUS-ETS

First, we performed PCR using primer Set A and cDNA from cell lines expressing either *EWSR1-FLII* (NCR-EW2), *EWSR1-ERG* (WES), or *EWSR1-ETV4* (NCR-EW3) and diluted plasmid vectors (10^4 molecules) containing *EWSR1-ETV1*, *EWSR1-FEV*, *FUS-ERG*, and *FUS-FEV* (Fig. 2a). A PCR product with expected length was identified in each reaction without recognizable background. Similarly, fusion genes with the expected length were amplified by PCR using Set B primers (Fig. 2b). In all cases, only a single band was detected with low background. All PCR products amplified with either Set A or Set B were sequenced successfully using the forward or reverse primer mix. Sequence analysis showed that all PCR products were the expected sequences of the *EWSR1/FUS-ETS* variants.

Next, we examined the sensitivity of the PCR. We performed RT–PCR using Set A primers and cDNA from cell lines expressing either *EWSR1-FLII*, *EWSR1-ERG*, or *EWSR1-ETV4*. We detected the respective fusion genes from cDNA equivalent to 100 pg of RNA using 35 cycles, according to the cycle number of the existing analysis (Supplementary Fig. S1). RT–PCR using Set B primers had comparable sensitivity with RT–PCR using Set A primers (Supplementary Fig. S1). For fusion transcripts without cell lines, we used a dilution series of plasmid vectors. Using Set A primers, positive results were obtained with 10^2 plasmid molecules for *EWSR1-ETV1* and *FUS-ERG*, and 10^3 molecules for *EWSR1-FEV* and *FUS-FEV* (Supplementary Fig. S2). The sensitivity of Set B was comparable with that of Set A. Similarly, we performed the PCR at 40 cycles, and obtained a clear band with less template (data not shown).

Detection of EWSR1/FUS-ETS in clinical samples

We examined the usefulness of these primer sets using clinical samples. We utilized frozen material from Ewing sarcoma diagnosed morphologically, immunohistochemically, and genetically. Specifically, six small round cell tumors with membranous CD99-positivity and

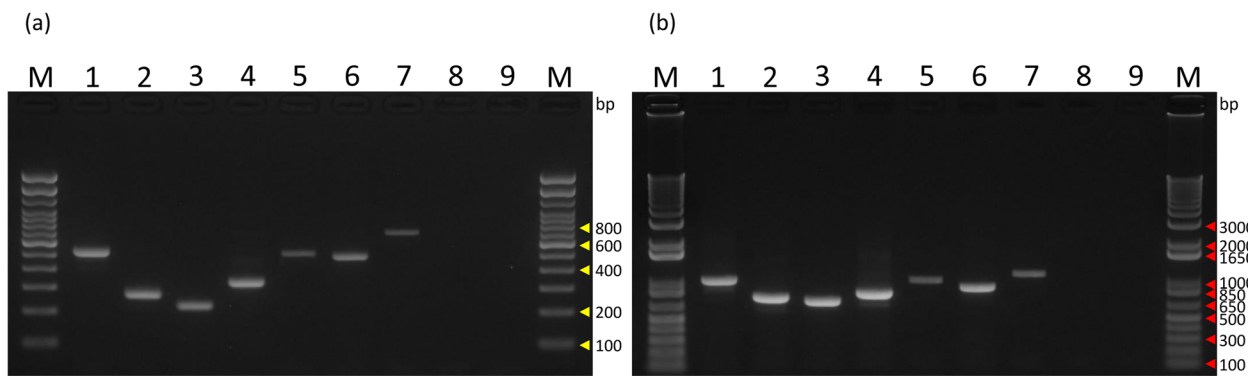


Fig. 2 Specificity of multiplex primers to each fusion gene. Multiplex PCR for *EWSR1/FUS-ETS* transcript variants using Set A (a) and Set B (b) primers. Lane M: Trackit 100-bp ladder marker (a) or Trackit 1-kbp plus ladder (b). Molecular sizes are indicated in the right with yellow arrowheads (a) and red arrowheads (b), respectively.; lane 1: NCR-EW2 cDNA (*EWSR1-FLI1*); lane 2: WES cDNA (*EWSR1-ERG*); lane 3: *EWSR1-ETV1* plasmid; lane 4: NCR-EW3 cDNA (*EWSR1-ETV4*); lane 5: *EWSR1-FEV* plasmid; lane 6: *FUS-ERG* plasmid; lane 7: *FUS-FEV* plasmid; lane 8: HEK293 cDNA; lane 9: no template control. The plasmid samples contained the same amount of HEK293 cDNA as the Ewing cell lines

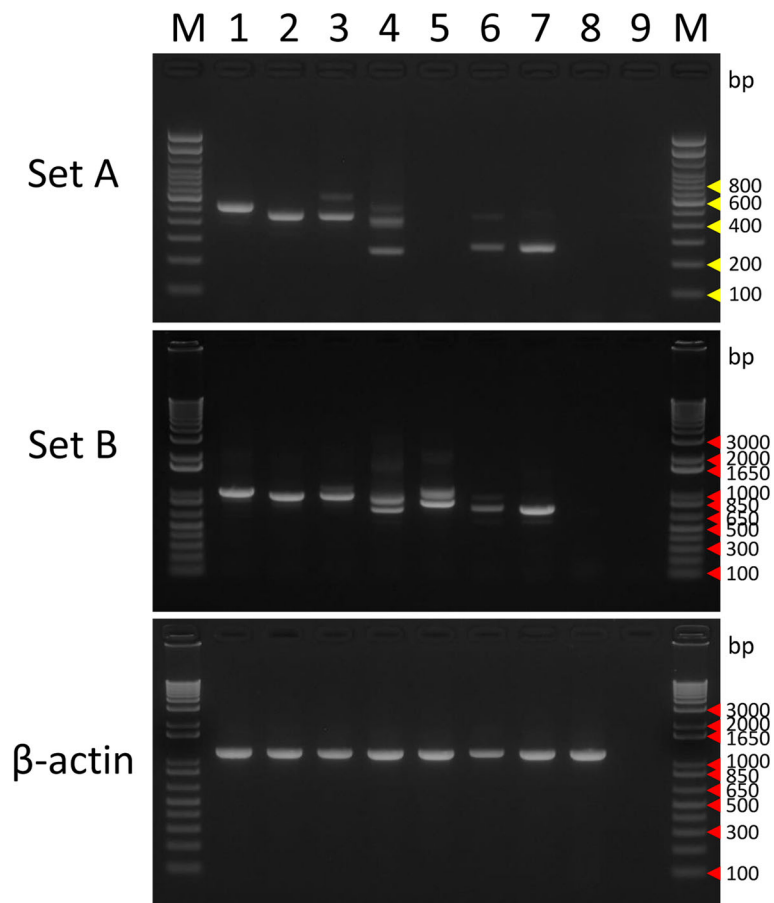


Fig. 3 Multiplex RT-PCR in tumor samples. Multiplex (top and middle panels) and control (bottom panel) RT-PCR were performed in six tumor samples. Lane M: Trackit 100-bp ladder marker (top panel) or Trackit 1-kbp plus ladder (middle and bottom panels). Molecular sizes are indicated in the right with yellow arrowheads (a) and red arrowheads (b), respectively.; lane 1: NCR-EW2 cDNA for the positive control; lane 2: tumor 1; lane 3: tumor 2; lane 4: tumor 3; lane 5: tumor 4; lane 6: tumor 5; lane 7: tumor 6; lane 8: NRS-1 cDNA for the negative control; lane 9: no template control

EWSR1 rearrangement by FISH or RT–PCR were analyzed. The fusion gene of tumor 4 was not detected by existing RT–PCR. Using Set A, we detected *EWSR1/FUS-ETS* in five of six cases (Fig. 3). Sequence analysis confirmed that tumors 1 and 2 had *EWSR1-FLI1*, tumor 3 had *EWSR1-FEV*, and tumors 5 and 6 had *EWSR1-ERG* (Table 2). Using PCR with Set B, we identified *EWSR1/FUS-ETS* in all six cases (Fig. 3). We detected three bands in tumor 4 using Set B primers. Sequence analysis revealed that these bands were *EWSR1-ERG*, but the fusion point was unclear because of multiple PCR products. Accordingly, we examined this fusion gene in detail and reviewed the clinicopathological features of this case.

A unique case of an *EWSR1-ERG*-expressing tumor

Clinical and pathological characteristics

We reviewed the clinical and pathological characteristics. The patient was a 15-year-old male with a history of acute lymphoblastic leukemia who presented with a mass measuring 1.5 × 1.0 × 0.7 cm in his nasal vestibule. The tumor was subjected to excisional biopsy. Histologically, the tumor exhibited diffuse proliferation of undifferentiated cells (Fig. 4a) with round to oval nuclei and a moderate amount of cytoplasm with a clear cell border. Focally, the tumor cells proliferated with fibrous to myxoid stroma (Fig. 4b) and were positive for Periodic acid–Schiff (PAS) staining in the cytoplasm (Fig. 4c). Immunohistochemically, tumor cells demonstrated membranous positivity for CD99, positivity for Nkx2.2 (Fig. 4d and e), focal positivity for S100 and negativity for desmin, myogenin, MyoD1, cytokeratin (AE1/AE3), CD31, CD34, CD3, CD20, and CD1a. FISH analysis of fresh-tissue touch preparations detected *EWSR1* split signals in most tumor cells but not *FUS* split signals (Fig. 4f). The tumor had consistent features of Ewing sarcoma based on CD99 positivity and *EWSR1* rearrangement, although the histological picture was somewhat unusual in that it showed focal myxoid stroma.

Table 2 Fusion transcripts identified in tumor samples

Tumor	Fusion Transcripts ^a
1	<i>EWSR1</i> exon 7 - <i>FLI1</i> exon 6 (fusion variant 11)
2	<i>EWSR1</i> exon 7 - <i>FLI1</i> exon 6 (fusion variant 11)
3	<i>EWSR1</i> exon 7 - <i>FEV</i> exon 2 (fusion variant 24), <i>EWSR1</i> Δexon 8 (c.794 to 943)- <i>FEV</i> exon 2
4	<i>EWSR1</i> Δexon 6 (c.414 to 522) - intron 6 - intron 6 / <i>ERG</i> intron 8 - exon 9
5	<i>EWSR1</i> exon 7 - <i>ERG</i> exon 12 (fusion variant 19)
6	<i>EWSR1</i> exon 7 - <i>ERG</i> exon 12 (fusion variant 19)

^aOnly the in-frame fusions are described here. The fusion variant numbers in Fig. 1 are shown in parentheses.

Detailed analysis of the fusion transcript

Sequence analysis of the multiplex PCR product revealed that the fusion gene was *EWSR1-ERG*. To determine the sequence of the individual products, we performed another PCR assay using *EWSR1* exon 4 and *ERG* exon 12 primers, and the products were subcloned into the pGEM-T vector and sequenced. We identified four transcript variants, and the most frequent one was in-frame (Fig. 5). The major in-frame *EWSR1-ERG* fusion transcript variant included a partial sequence of exon 6 (c.414 to c.522), two cryptic exons (c.581 + 55 to + 90, c.581 + 227 to + 369) in intron 6 of *EWSR1*, a cryptic exon in intron 8 of *ERG* (c.767–214 to – 198), and exon 9 of *ERG* (Fig. 5 and Supplementary Fig. S3a, b and c). All four variants had identical sequences from *ERG*. Three out-of-frame variants were thought to be produced by differential splicing within *EWSR1* (Fig. 5 and Supplementary Fig. S3a, b and c).

*Genomic structure of the *EWSR1-ERG* fusion*

To clarify whether the rare variants were derived from alternative splicing or different breakpoints in genomic DNA, we performed genomic PCR and identified a single fused sequence showing that intron 6 of *EWSR1* was joined to intron 8 of *ERG* (Fig. 6). The genomic fusion point was identical to the fusion points in transcripts, indicating a part of *EWSR1* intron 6 and a short sequence of *ERG* intron 8 formed a cryptic exon collectively. Notably, all flanking sequences of all cryptic exons followed the GU/AG mRNA splicing rule, and all four transcript variants were supposed to be derived from alternative splicing.

Discussion

We developed a novel RT–PCR assay that can efficiently detect both *EWSR1-ETS* and *FUS-ETS* observed in Ewing sarcoma. We identified *EWSR1/FUS-ETS* fusion transcripts in all cell lines and pathologically defined Ewing sarcoma tumors that were tested. The appropriately designed primers enabled the detection of various fusion variants in a single round of PCR. Additionally, the identified transcripts were successfully sequenced by mixed forward or reverse primers in each case. Among 28 *EWS/FUS-ETS* variants reported so far, we detected five using cell lines and tumor tissues, and additionally, we identified a novel variant.

We were able to detect the fusion genes from 100 pg of total RNA from cell lines. In addition, we detected 1000 molecules of the fusion gene in a PCR reaction. For clinical samples, we use 1/40 of the cDNA synthesized with 1 μg of total RNA as the PCR template. Assuming that the amount of total RNA per cell is 0.01 ng, the template used for PCR is theoretically equivalent to 2500 cells. Thus, although the number of samples

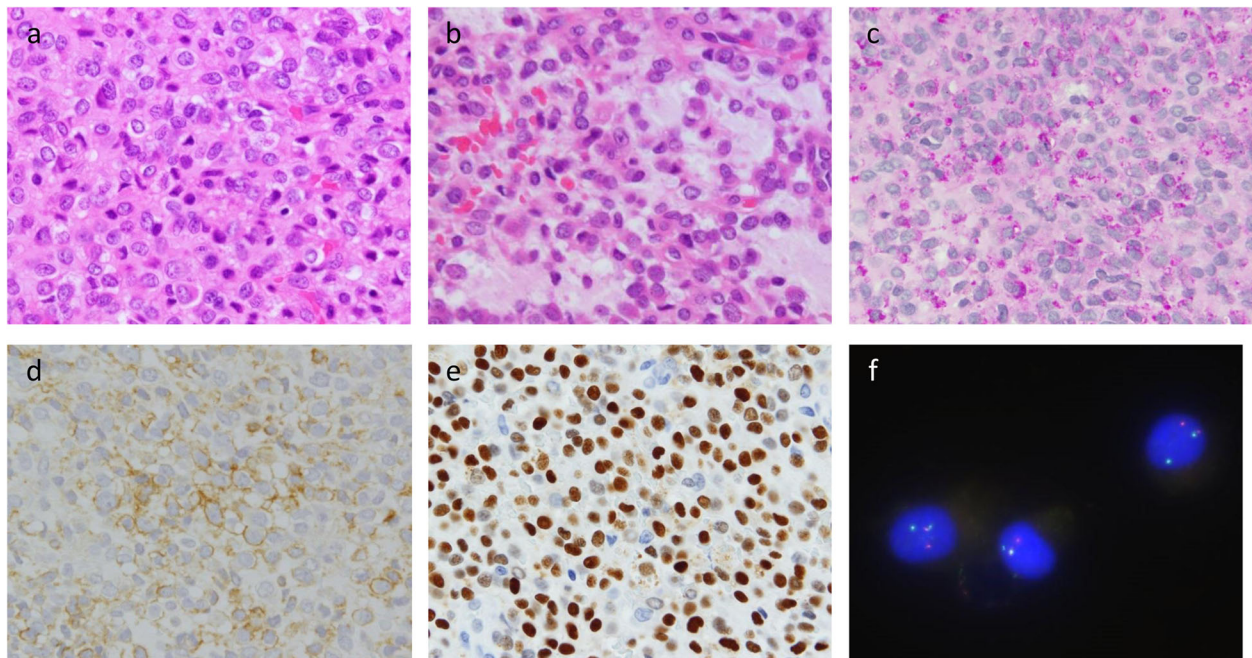


Fig. 4 Pathological features of the tumor and FISH analysis. The pathological features of tumor 4 are shown. **a, b** Hematoxylin and eosin staining. **c** PAS staining. **d** Immunohistochemistry of CD99. **e** Immunohistochemistry of Nkx2.2. **f** FISH analysis using the *EWSR1* break-apart probe

analyzed was small, our method is theoretically applicable to clinical tumor samples.

In 1995, Downing et al. reported multiplex RT-PCR for the detection of *EWSR1-FLI1* and *PAX3-FOXO1* to differentiate Ewing sarcoma and alveolar rhabdomyosarcoma [19]. However, many fusion variants were discovered afterwards. In addition, the primers they used cannot detect fusion variants with a short N-terminal sequence. In 2001, Peter et al. used a real-time PCR

system to discriminate Ewing sarcoma, alveolar rhabdomyosarcoma, synovial sarcoma, and small round cell desmoplastic tumor [20]. They used primers only for *EWSR1-ETS*. As they utilized a common *EWSR1* probe for the detection of the amplicon, they were unable to differentiate fusion gene combinations. Moreover, the product sizes were too large for the real-time PCR method. Yoshino et al. reported the simultaneous detection of *EWSR1-ETS* in 2003 [21]. They used Bioanalyzer

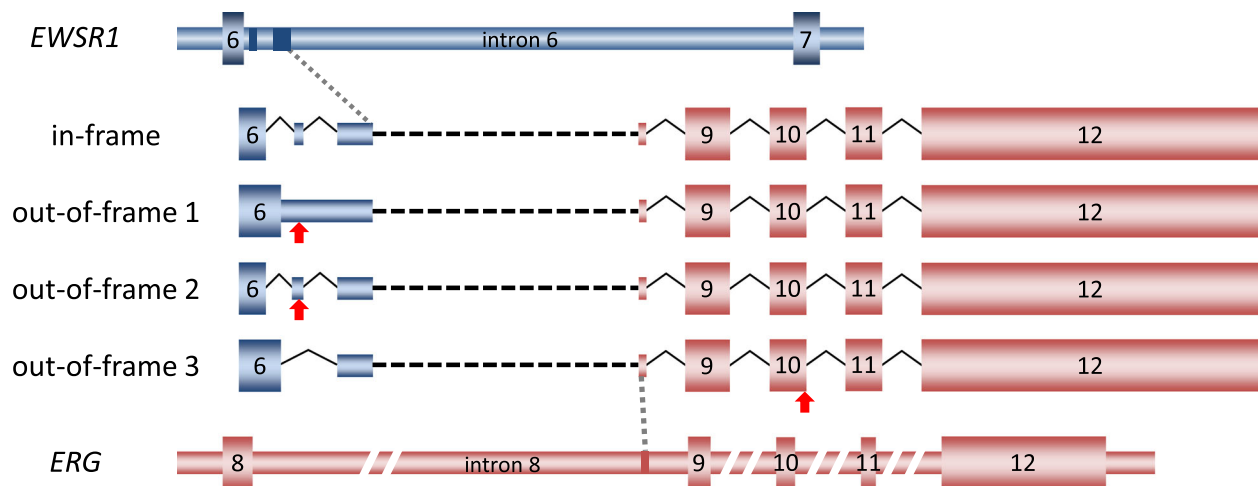
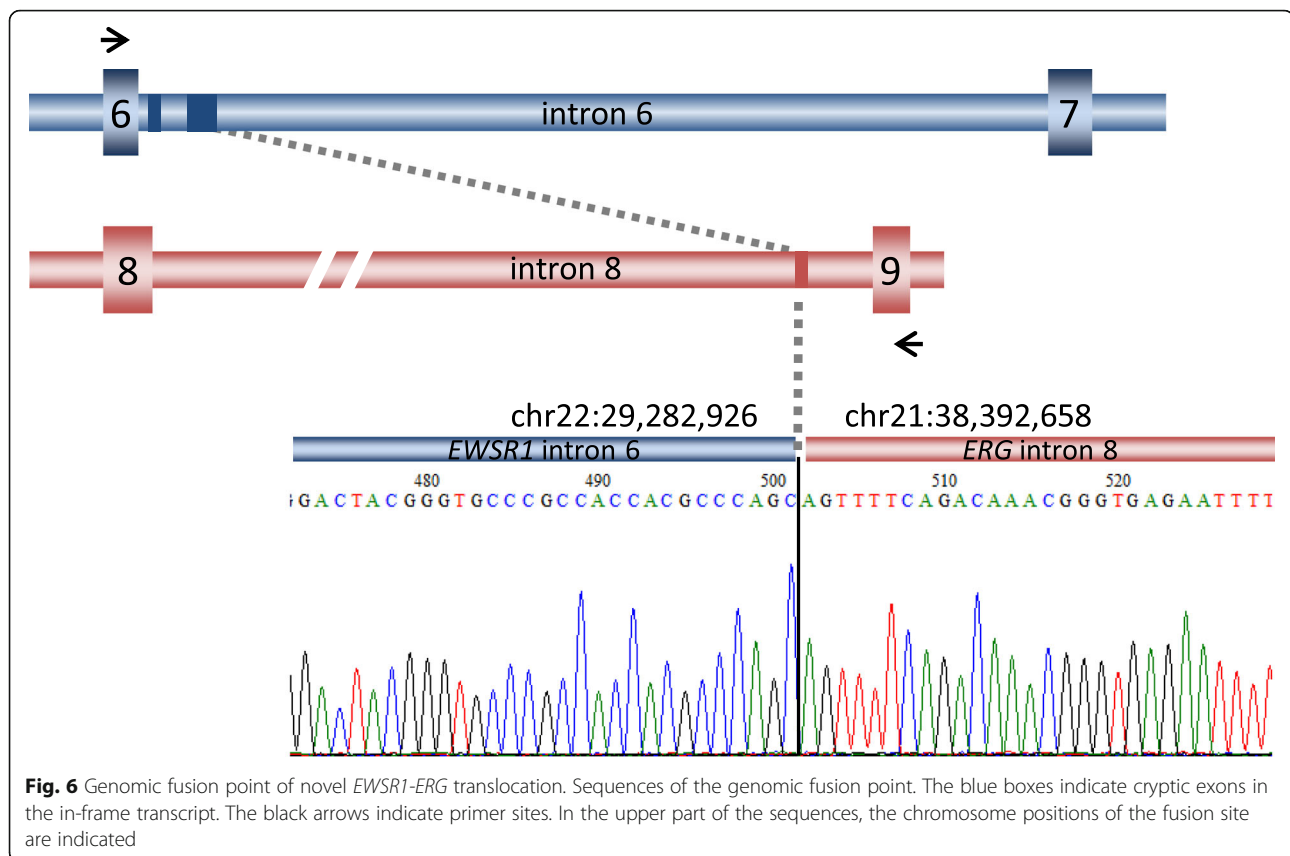


Fig. 5 Schematic representations of the fusion transcripts in tumor 4. Scheme of the transcript variants of *EWSR1-ERG*. The blue boxes in intron 6 of *EWSR1* and red box in intron 8 of *ERG* indicate cryptic exons found in the in-frame variant. The red arrows in out-of-frame variants are sites of the termination codon. *EWSR1* and *ERG* are connected by black dotted lines



to confirm the product length, which made it possible to predict the gene and exon combinations, but they utilized *EWSR1* exon 7 primer and were unable to detect fusion with a short N-terminal sequence. Thus, none of these assays were able to detect *FUS-ETS* fusions. In routine pathological practice, Ewing sarcoma with atypical morphology or small round cell sarcoma without typical *EWSR1/FUS-ETS* fusions is occasionally observed. Therefore, rapid detection of all Ewing sarcoma related fusions is useful in clinical settings. The advantages of conventional RT-PCR with gel electrophoresis are that it is inexpensive and not laborious, and the length of the product can be recognized. In addition, all the processes can be performed without special equipment such as a real-time PCR system or next-generation sequencer. The standard break-apart FISH method takes 2 days to determine *EWSR1* and *FUS* rearrangement [29], and it takes another 2 days to determine the fusion partner. However, our method enables confirmation of the presence of the *EWSR1/FUS-ETS* fusion gene in 5.5 h and determination of the sequence in approximately 10 h.

Furthermore, we reported a case of Ewing sarcoma with atypical histological features whose fusion transcript completely lacked exon 7 of *EWSR1*. By our

methods, the use of the *EWSR1* upstream forward primer enabled the detection of a transcript variant with an unexpectedly shorter N-terminal region of *EWSR1*. Many laboratories detect fusion genes by RT-PCR, but most primers reported thus far cannot amplify fusion transcripts lacking *EWSR1* exon 7. Thus, false-negative results may occur with *EWSR1-ETS* and *EWSR1-ERG*. Therefore, when Ewing sarcoma is pathologically suspected, but all seven types of known fusion genes are negative, analysis using an *EWSR1* primer upstream of exon 7 should be considered.

Conclusions

We developed a multiplex PCR assay method that is simple, accurate, and efficient to detect fusion genes observed in Ewing sarcoma. Our assay will aid in the rapid and accurate diagnosis of Ewing sarcoma. We also identified a novel fusion variant with a short N-terminal region that may have been previously overlooked. This highlights why the RT-PCR primers for the genetic diagnosis of Ewing sarcoma should be optimized.

Abbreviations

RT-PCR: Reverse transcription-polymerase chain reaction; FISH: Fluorescence in situ hybridization; PAS: Periodic acid-Schiff

Supplementary Information

The online version contains supplementary material available at <https://doi.org/10.1186/s13000-021-01164-6>.

Additional file 1: Supplementary Table S1. List of antibodies.

Additional file 2: Supplementary Table S2. Sequences of genomic PCR and sequencing primers.

Additional file 3: Supplementary Fig. S1. Detection sensitivity of primers for *EWSR1-ETS* cDNA. Serial dilutions of cDNA from Ewing sarcoma cell lines were amplified by Set A (upper panel) or Set B primers (lower panel). Lane M: Trackit100-bp ladder marker (upper panel, yellow arrowhead) or Trackit1-kbp plus ladder (lower panel, red arrowhead), molecular marker sizes are indicated in the left; lane 1: template cDNA corresponding to 10 ng to total RNA; lane 2: 1 ng; lane 3: 100 pg; lane 4: 10 pg; lane 5: 1 pg; lane 6: 0.1 pg; lane 7: no template control.

Additional file 4: Supplementary Fig. S2. Detection sensitivity of primers for *EWSR1-ETS* plasmids. Serial dilutions of *EWSR1/FUS-ETS*-containing plasmids were amplified using primer Set A (upper panels) and Set B (lower panels). We estimated the molecular weight from the size of each plasmid, and made serial dilution of the respective plasmids and used 105 to 100 molecules as a starting template in 25 μ l of the PCR reaction mix. Lane M: Trackit100-bp ladder marker (upper panel, yellow arrowhead) or Trackit1-kbp plus ladder (lower panel, red arrowhead), molecular marker sizes are indicated in the left; lane 1: 105 molecules; lane 2: 104 molecules; lane 3: 103 molecules; lane 4: 102 molecules; lane 5: 101 molecules; lane 6: 100 molecule; lane 7: no template control.

Additional file 5: Supplementary Fig. S3. Scheme of alternative splicing and sequence in novel *EWSR1-ERG* transcripts. (a) Scheme of exon 6 and first 369 bases of intron 6 of *EWSR1*. The splicing patterns of the in-frame variant are represented by red lines and a red number. The splicing sites shared by some variants are denoted by black numbers. The two blue bars under intron 6 are cryptic exonic regions of the in-frame variant. The splicing patterns of the two out-of-frame variants are shown in purple and green, respectively. No sequence was spliced out in one variant. (b) Sequences of *EWSR1* exon 6 and intron 6 (c.581 + 1 to + 393) and alternative splicing sites. The genomic location numbers are based on the GRCh37/hg19 version. The boldfaced sequences represent truncated exon 6 (c.414 to c.522). The sequences corresponding to the cryptic exon in intron 6 are underlined. GT/gt (green character): splice donor sites, ag (red character): splice acceptor sites. Sites involved in splicing are numbered in the upper part of the sequences. (c) Sequences of *ERG* intron 8 (c.767–1 to – 230) and exon 9 and alternative splicing sites. The genomic location numbers and sites involved in splicing are shown as in (b).

Acknowledgments

The authors thank Michiko Tatsuno, MS, and Ms. Hiromi Ono for their technical assistance.

Authors' contributions

HU-Y and HO contributed to the conception, design, data curation, visualization of this work and writing the manuscript. HU-Y established methodology and performed investigation. KN supported the experiment. HO, TY and AN performed the evaluation of pathology. CK, MK and KM contributed to the collection of samples. NK provided laboratory infrastructure. All authors read and approved the final manuscript.

Funding

This work was supported in part by a grant from the National Center for Child Health and Development (2019C-3, 30E-2) and AMED under Grant Number JP19ck0106333. The funders had no role in the study design, data collection, and analysis, decision to publish, or preparation of the manuscript.

Availability of data and materials

Not applicable.

Declarations

Ethics approval and consent to participate

All specimens and clinical data were obtained with either informed written consent or a formal waiver of consent under protocols approved by the ethics committee/IRB at the National Center for Child Health and Development (No. 1035).

Consent for publication

Not applicable.

Competing interests

The authors declare no competing financial interests.

Author details

¹Department of Pediatric Hematology and Oncology Research, National Research Institute for Child Health and Development, Tokyo 157-8535, Japan. ²Division of Diagnostic Pathology, Keio University School of Medicine, Tokyo 160-8582, Japan. ³Department of Pathology, Keio University School of Medicine, Tokyo 160-8582, Japan. ⁴Department of Pathology, National Center for Child Health and Development, Tokyo 157-8535, Japan. ⁵Children's Cancer Center, National Center for Child Health and Development, Tokyo 157-8535, Japan. ⁶Department of Pediatrics, Graduate School of Medicine, University of Tokyo, Tokyo 113-8655, Japan. ⁷Department of Clinical Research, Saitama Children's Medical Center, Saitama, Saitama 330-8777, Japan.

Received: 14 July 2021 Accepted: 18 October 2021

Published online: 08 November 2021

References

- Turc-Carel C, Philip I, Berger MP, Philip T, Lenoir GM. Chromosome study of Ewing's sarcoma (ES) cell lines. Consistency of a reciprocal translocation t(11;22)(q24;q12). *Cancer genet. Cytogenet.* 1984;12(1):1–19. [https://doi.org/10.1016/0165-4608\(84\)90002-5](https://doi.org/10.1016/0165-4608(84)90002-5).
- Sorensen PH, Lessnick SL, Lopez-Terrada D, Liu XF, Triche TJ, Denny CT. A second Ewing's sarcoma translocation, t(21;22), fuses the EWS gene to another ETS-family transcription factor. *ERG Nat Genet.* 1994;6(2):146–51. <https://doi.org/10.1038/ng0294-146>.
- Jeon IS, Davis JN, Braun BS, Sublett JE, Roussel MF, Denny CT. A variant Ewing's sarcoma translocation (7;22) fuses the EWS gene to the ETS gene ETV1. *Oncogene.* 1995;10(6):1229–34.
- Urano F, Umezawa A, Hong W, Kikuchi H, Hata J. A novel chimera gene between EWS and E1A-F, encoding the adenovirus E1A enhancer-binding protein, in extraosseous Ewing's sarcoma. *Biochem Biophys Res Commun.* 1996;219(2):608–12. <https://doi.org/10.1006/bbrc.1996.0281>.
- Peter M, Couturier J, Pacquement H, Michon J, Thomas G, Magdelenat H, et al. A new member of the ETS family fused to EWS in Ewing tumors. *Oncogene.* 1997;14(10):1159–64. <https://doi.org/10.1038/sj.onc.1200933>.
- Sankar S, Lessnick SL. Promiscuous partnerships in Ewing's sarcoma. *Cancer Genet.* 2011;204(7):351–65. <https://doi.org/10.1016/j.cancergen.2011.07.008>.
- Shing DC, McMullan DJ, Roberts P, Smith K, Chin SF, Nicholson J, et al. FUS/ERG gene fusions in Ewing's tumors. *Cancer Res.* 2003;63(15):4568–76.
- Ng TL, O'Sullivan MJ, Pallen CJ, Hayes M, Clarkson PW, Winstanley M, et al. Ewing sarcoma with novel translocation t(2;16) producing an in-frame fusion of FUS and FEV. *J. Mol. Diagn.* 2007;9(4):459–63. <https://doi.org/10.2353/jmoldx.2007.070009>.
- Delattre O, Zucman J, Plougastel B, Desmaziere C, Melot T, Peter M, et al. Gene fusion with an ETS DNA-binding domain caused by chromosome translocation in human tumours. *Nature.* 1992;359:162–5. <https://doi.org/10.1038/359162a0>.
- Zucman J, Melot T, Desmaziere C, Ghysdael J, Plougastel B, Peter M, et al. Combinatorial generation of variable fusion proteins in the Ewing family of tumours. *EMBO J.* 1993;12(12):4481–7. <https://doi.org/10.1002/j.1460-2075.1993.tb06137.x>.
- Riggi N, Knoechel B, Gillespie SM, Rheinbay E, Boulay G, Suvà ML, et al. EWS-FLI1 utilizes divergent chromatin remodeling mechanisms to directly activate or repress enhancer elements in Ewing sarcoma. *Cancer Cell.* 2014; 26(5):668–81. <https://doi.org/10.1016/j.ccell.2014.10.004>.
- de Alava E, Lessnick SL, Stamenkovic I. Ewing Sarcoma. In: WHO Classification of Tumours Editorial Board, Soft Tissue and Bone Tumours.

- Lyon: International Agency for Research on Cancer; 2020. p. 323–5. (WHO Classification of Tumours series, 5th ed.: vol. 3).
13. Vargas AC, Selinger CI, Satgunaseelan L, Cooper WA, Gupta R, Stalley P, et al. Atypical Ewing sarcoma breakpoint region 1 fluorescence in-situ hybridization signal patterns in bone and soft tissue tumours: diagnostic experience with 135 cases. *Histopathology*. 2016;69(6):1000–11. <https://doi.org/10.1111/his.13031>.
 14. Ladanyi M, Gerald W. Fusion of the EWS and WT1 genes in the desmoplastic small round cell tumor. *Cancer Res*. 1994;54(11):2837–40.
 15. Rabbitts TH, Forster A, Larson R, Nathan P. Fusion of the dominant negative transcription regulator CHOP with a novel gene FUS by translocation t(12;16) in malignant liposarcoma. *Nat Genet*. 1993;4(2):175–80. <https://doi.org/10.1038/ng0693-175>.
 16. Fujimura Y, Ohno T, Siddique H, Lee L, Rao VN, Reddy ES. The EWS-ATF-1 gene involved in malignant melanoma of soft parts with t(12;22) chromosome translocation, encodes a constitutive transcriptional activator. *Oncogene*. 1996;12(1):159–67.
 17. Waters BL, Panagopoulos I, Allen EF. Genetic characterization of angiomatoid fibrous histiocytoma identifies fusion of the FUS and ATF-1 genes induced by a chromosomal translocation involving bands 12q13 and 16p11. *Cancer Genet Cytogenet*. 2000;121(2):109–16. [https://doi.org/10.1016/S0165-4608\(00\)00237-5](https://doi.org/10.1016/S0165-4608(00)00237-5).
 18. Brandal P, Panagopoulos I, Bjerkehagen B, Gorunova L, Skjeldal S, Micci F, et al. Detection of a t(1;22)(q23;q12) translocation leading to an EWSR1-PBX1 fusion gene in a myoepithelioma. *Genes Chromosomes Cancer*. 2008;47(7):558–64. <https://doi.org/10.1002/gcc.20559>.
 19. Downing JR, Khandekar A, Shurtleff SA, Head DR, Parham DM, Webber BL, et al. Multiplex RT-PCR assay for the differential diagnosis of alveolar rhabdomyosarcoma and Ewing's sarcoma. *Am J Pathol*. 1995;146(3):626–34.
 20. Peter M, Gilbert E, Delattre O. A multiplex real-time pcr assay for the detection of gene fusions observed in solid tumors. *Lab Invest*. 2001;81(6):905–12. <https://doi.org/10.1038/labinvest.3780299>.
 21. Yoshino N, Kojima T, Asami S, Motohashi S, Yoshida Y, Chin M, et al. Biological and Diagnostic Significance and clinical applications of chimeric genes in Ewing's sarcoma. *Biol. Pharm. Bull*. 2003;26:585–8. <https://doi.org/10.1248/bpb.26.585>.
 22. Patócs B, Németh K, Garami M, Arató G, Kovalszky I, Szendroi M, et al. Utilisation of fluorescent multiplex PCR and laser-induced capillary electrophoresis for the diagnosis of Ewing family of tumours in formalin-fixed paraffin-embedded tissues. *J Clin Pathol*. 2012;65(12):1112–8. <https://doi.org/10.1136/clinpath-2012-201154>.
 23. Urano F, Umezawa A, Yabe H, Hong W, Yoshida K, Fujinaga K, et al. Molecular analysis of Ewing's sarcoma: another fusion gene, EWS-E1AF, available for diagnosis. *Jpn J Cancer Res*. 1998;89(7):703–11. <https://doi.org/10.1111/j.1349-7006.1998.tb03274.x>.
 24. Ogoe A, Motoyama T, Hotta T, Watanabe H. In vitro differentiation and proliferation in a newly established human rhabdomyosarcoma cell line. *Virchows Arch*. 1995;426(4):385–91. <https://doi.org/10.1007/bf00191348>.
 25. Ueno-Yokohata H, Okita H, Nakasato K, Akimoto S, Hata J, Koshinaga T, et al. Consistent in-frame internal tandem duplications of BCOR characterize clear cell sarcoma of the kidney. *Nat Genet*. 2015;47(8):861–3. <https://doi.org/10.1038/ng.3338>.
 26. Kovar H, Jugovic D, Melot T, Zoubek A, Lenoir G, Fink FM, et al. Cryptic exons as a source of increased diversity of Ewing tumor-associated EWS-FLI1 chimeric products. *Genomics*. 1999;60(3):371–4. <https://doi.org/10.1006/geno.1999.5919>.
 27. Peter M, Mugneret F, Aurias A, Thomas G, Magdelenat H, Delattre O. An EWS/ERG fusion with a truncated N-terminal domain of EWS in a Ewing's tumor. *Int J Cancer*. 1996;67(3):339–42. [https://doi.org/10.1002/\(SICI\)1097-0215\(19960729\)67:3<339::AID-IJC6>3.0.CO;2-S](https://doi.org/10.1002/(SICI)1097-0215(19960729)67:3<339::AID-IJC6>3.0.CO;2-S).
 28. Gamberi G, Cocchi S, Benini S, Magagnoli G, Morandi L, Kreshak J, et al. Molecular diagnosis in Ewing family tumors: the Rizzoli experience—222 consecutive cases in four years. *J Mol Diagn*. 2011;13(3):313–24. <https://doi.org/10.1016/j.jmoldx.2011.01.004>.
 29. Trautmann M, Hartmann W. Molecular approaches to diagnosis in Ewing sarcoma: fluorescence in situ hybridization (FISH). *Methods Mol Biol*. 2021;2226:65–83. https://doi.org/10.1007/978-1-0716-1020-6_6.

Publisher's Note

Springer Nature remains neutral with regard to jurisdictional claims in published maps and institutional affiliations.

Ready to submit your research? Choose BMC and benefit from:

- fast, convenient online submission
- thorough peer review by experienced researchers in your field
- rapid publication on acceptance
- support for research data, including large and complex data types
- gold Open Access which fosters wider collaboration and increased citations
- maximum visibility for your research: over 100M website views per year

At BMC, research is always in progress.

Learn more biomedcentral.com/submissions

